ELSEVIER

Chemical Engineering Journal 90 (2002) 185–193

Chemical Engineering Journal

www.elsevier.com/locate/cej

Langmuir–Hinshelwood–Hougen–Watson rate equations for the transalkylation of methylamines

N. Staelens, M.-F. Reyniers, G.B. Marin*

Laboratorium voor Petrochemische Techniek, Ghent University, Krijgslaan 281 S5, B-9000 Ghent, Belgium

Abstract

The transalkylation of methylamines over a commercial amorphous silica-alumina catalyst was investigated. Intrinsic kinetic experiments have been performed in an integral plug flow reactor at temperatures ranging from 623 to 683 K and pressures ranging from 0.2 to 2 MPa. A Langmuir–Hinshelwood–Hougen–Watson model for the transalkylation reactions was developed, describing adequately the experimental data over the investigated range of conditions. The model is based on three dual-site surface reactions as rate-determining steps and quasi-equilibrated adsorption–desorption of ammonia and the methylamines. The equilibrium coefficients of the latter are of the same order of magnitude. A significant fraction of the catalyst surface remains uncovered.

Keywords: Methylamines; Kinetics; Elementary reactions; Hougen–Watson equations; Transalkylation

1. Introduction

Methylamines represent important chemical intermediates for the synthesis of nitrogen-containing organic compounds. The industrial synthesis of methylamines is performed in a multi-bed adiabatic reactor via the exothermic reaction of methanol and ammonia over amorphous oxide catalysts, such as alumina or silica-alumina. Typical reaction conditions range from 623 to 723 K and 0.5 to 3 MPa. The nitrogen to carbon ratio ranges from 0.65 to 5 mol mol^{-1}. In these conditions, the reaction proceeds to a thermodynamic equilibrium mixture of ammonia, monomethylamine, dimethylamine and trimethylamine. The conversion of methanol is almost complete. The equilibrium distribution favors the formation of trimethylamine, while dimethylamine is commercially the most attractive [1]. Once formed, ammonia and the methylamines may react via transalkylation reactions such as:

$$2CH_3NH_2 = NH_3 + (CH_3)_2NH \quad (1)$$

$$2(CH_3)_2NH = CH_3NH_2 + (CH_3)_3N \quad (2)$$

$$NH_3 + (CH_3)_3N = CH_3NH_2 + (CH_3)_2NH \quad (3)$$

Depending on the market demand, trimethylamine and/or monomethylamine are usually recycled together with the excess ammonia, to obtain an increased yield of dimethylamine. However, separation and reequilibration of trimethylamine is costly and energy intensive. Hence, understanding the kinetics of the transalkylation reactions is a must to optimize the production of dimethylamine.

Several authors [2–5] investigated the kinetics of the overall synthesis of methylamines. Issoire and van Long [6] have investigated the thermodynamics of the transalkylation reactions. However, only two reports propose reaction rate equations for the transalkylation. Restelli and Coull [7] investigated the initial reaction rates of monomethyl and dimethylamine over montmorillonite. The studied total pressure varied from 0.014 to 0.106 MPa. It was found that the rate of disappearance of monomethylamine was proportional to the partial pressure of monomethylamine in the temperature range from 593 to 644 K. The rate of disappearance of dimethylamine was found to be proportional to the square root of the partial pressure of dimethylamine for temperatures between 522 and 566 K. Only rate equations for the disappearance of monomethyl and dimethylamine were given. No production rates were considered and experiments were performed at low pressure only. Mitchell et al. [8], investigating the transalkylation reactions at 1.8 MPa and between 573 and 601 K, found that a simple power rate law describes the kinetics quite well. For a better understanding of the transalkylation reactions, however, a more fundamental approach taking into account the catalyst is required.

Our goal was to develop a kinetic model describing the transalkylation reactions in the pressure and temperature range industrially used, based on elementary steps involving

Abbreviations: DMA, dimethylamine; FID, flame ionization detector; GC, gas chromatography; MMA, monomethylamine; TCD, thermal conductivity detector; TMA, trimethylamine

* Corresponding author. Tel.: +32-9-264-4517; fax: +32-9-264-4999.
E-mail address: guy.marin@rug.ac.be (G.B. Marin).

1385-8947/02/$ – see front matter
PII: S1385-8947(02)00079-7

Nomenclature

A	matrix
A_i	reparametrized pre-exponential factor (mol kg_{cat}^{-1} s^{-1})
$\boldsymbol{b}$	parameter vector
C	total number of key components
C_i	factor which is function of the standard reaction entropy for the adsorption of component i (MPa^{-1})
C_i^*	surface concentration of component i (mol m^{-2})
ΔH_i°	standard reaction enthalpy for the adsorption of component i (J mol^{-1})
$E_{a,i}$	activation energy of reaction i (J mol^{-1})
F_i	molar flow rate of component i (mol s^{-1})
$g_{i,k}$	model prediction of the kth response for experiment i
k_i	kinetic coefficient of reaction i (mol kg_{cat}^{-1} s^{-1})
$K_{a,i}$	adsorption equilibrium coefficient of component i (MPa^{-1})
$K_{eq,i}$	equilibrium coefficient of reaction i
L	total number of elements
M	total number of components
n	number of experiments
p_i	partial pressure of component i (MPa)
r_i	reaction rate of reaction i (mol kg_{cat}^{-1} s^{-1})
R	universal gas constant (8.314 J mol^{-1} K^{-1})
R	rank of a matrix
R_i	net production rate of component i (mol kg_{cat}^{-1} s^{-1})
S	objective function
T	temperature (K)
v	number of responses
W	weight of catalyst (kg_{cat})
$\boldsymbol{x}_i$	vector of experimental settings corresponding with experiment i
X_i	conversion of component i
y_i	mole fraction of component i
$y_{i,k}$	the ith experimental observation of the kth response

Greek symbols

σ^{kl}	the (k, l) element of the inverse of the covariance matrix of the experimental errors
ν	stoichiometric coefficient

Subscripts and superscripts

0	initial or inlet condition
cat	catalyst
dil	diluent
i	ith component
tot	total

adsorption, surface reaction and desorption. Therefore, intrinsic kinetic experiments have been performed in an integral high pressure plug flow reactor.

2. Experimental

2.1. Catalyst

The catalyst used was a commercial amorphous silica-alumina obtained from UCB Chemicals. The packed apparent bulk density was measured to be 0.74 g cm^{-3}. The surface area was found to be 3.52×10^5 m^2 kg^{-1}. The particle diameter used ranged from 0.3×10^{-3} to 0.7×10^{-3} m.

2.2. Experimental setup

The feed consisted of gaseous ammonia and liquid methylamines. Nitrogen was added in order to achieve the evaporation of the methylamines. Methylamines were obtained from UCB Chemicals. Ammonia and nitrogen were provided by Air Liquide. The mass flows of ammonia and methylamines were controlled by mass flow controllers from Bronkhorst (F1C0-FA-11-E, respectively, L2Z-FA-33-0). The mass flow of nitrogen was controlled by a Brooks 5850TR mass flow controller. After mixing and evaporation at 523 K, the gas stream was lead to the stainless steal reactor. The reactor was placed in a furnace and heated by infrared heaters. The inner tube in the reactor contains four thermocouples and three sample tubes (Fig. 1). The positions of the thermocouples can be set by the experimentator. Reactor pressure was controlled by a back pressure regulator valve. The reactor was filled with two catalytic beds separated by an inert bed of non-porous α-Al_2O_3 pellets of the same average diameter as the catalysts pellets. The catalyst bed was diluted with the same α-Al_2O_3 pellets in order to minimize temperature gradients in the reactor (dilution = 0.8 kg_{dil} $kg_{cat+dil}^{-1}$). At the inlet and the outlet of the reactor, an inert zone of α-Al_2O_3 pellets was provided to obtain an ideal plug flow and to preheat the gas mixture at reaction temperature. Samples were taken in the inert zone after each catalytic bed via the sample tubes 2 and 3 in the inner tube of the reactor (Fig. 1).

Based on correlations available in literature, inter- and intra-particle gradients [9–11] as well as radial and axial gradients on reactor scale were calculated [9]. Experiments were performed at such conditions that mass and heat transport limitations could be neglected and the reactor was operated under ideal plug flow conditions [12,13].

2.3. Analysis

The on-line gas analysis section contains a gas chromatograph HP 6890 equipped with two injection valves and thermal conductivity detector (TCD) and flame ionization detector (FID) detection. Separation of the components is

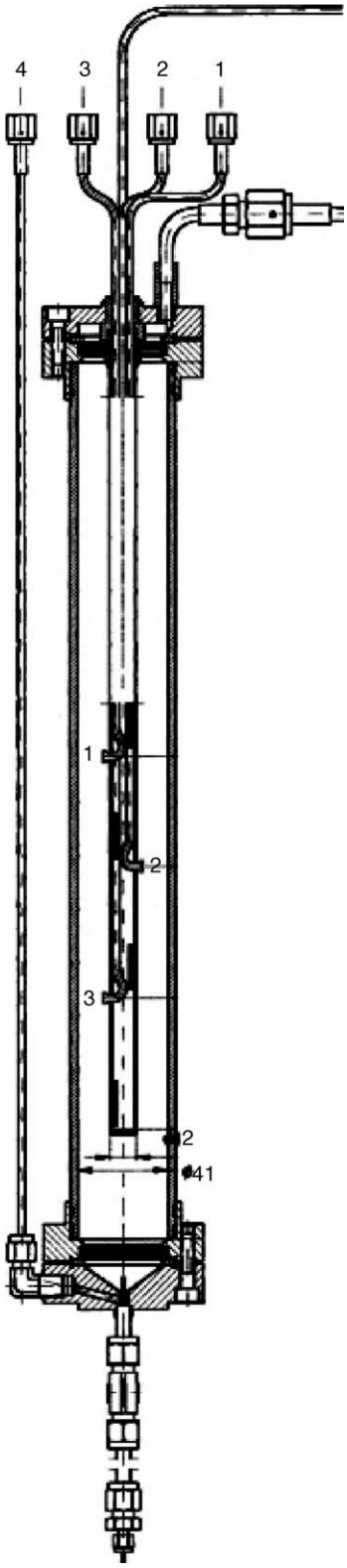

Fig. 1. Experimental reactor.

achieved by two CP-sil 5B capillary columns. The effluent composition, as analyzed by TCD detection was used to calculate mole fractions and conversions. FID detection was used to observe the formation of by-products. At higher temperatures (>673 K) the formation of C_2H_4, H_2, CH_4, as well as heavy nitrogen-containing compounds can occur next to the transalkylation reactions (Issoire and van Long [6], Schmitz [3]). Production of small amounts of by-products was observed only at the highest temperature (683 K) investigated. No deactivation of the catalyst has been observed.

3. Data evaluation

Nitrogen was also used as an internal standard in the gas chromatography (GC) analysis. Quantification of the product components was done by relating the peak surface areas to the flow rate of the internal standard. In each experiment, samples were taken during several hours to assure that steady-state conditions had been reached. Mass flow rates were normalized by the total mass balance for each analysis. Conversions were calculated by the direct method:

$$X_i = \frac{F_{i,0} - F_i}{F_{i,0}} \tag{4}$$

where X_i is the conversion of product i, F_i the normalized molar flow rate of i and $F_{i,0}$ the normalized initial flow rate. Mass, C, H and N balance closed between 95 and 105%. The amount of by-products was found to be negligible.

4. Modeling

Since the experimental reactor was operated integrally, a reactor model has to be considered in combination with a kinetic model. As mentioned previously, the experimental fixed bed reactor was operated in such a way that an ideal plug flow reactor model could be assumed. Since temperature and pressure gradients could be neglected too, it is sufficient to consider the continuity equations of the gas phase components. As the transalkylation reactions are equimolar, the mole fractions of the different components can then be calculated by integration of the following set of ordinary differential equations:

$$\frac{\mathrm{d}y_i}{\mathrm{d}(W/F_{\mathrm{tot},0})} = R_i \tag{5}$$

where y_i is the mole fraction of component i, W the total weight of the catalyst, $F_{\mathrm{tot},0}$ the total molar flow rate and R_i the net production rate of component i.

The integration of the set of ordinary differential equations was performed with the LSODA-subroutine [14,15] available at Netlib [16].

5. Regression analysis

Estimation of the kinetic parameters was performed by minimization of the objective function S:

$$S(\boldsymbol{b}) = \sum_{k=1}^{v}\sum_{l=1}^{v}\sigma^{kl}\sum_{i=1}^{n}[y_{i,k} - g_k(\boldsymbol{x}_i, \boldsymbol{b})][y_{i,l} - g_l(\boldsymbol{x}_i, \boldsymbol{b})] \rightarrow \text{minimum} \quad (6)$$

where S is the objective function, $\boldsymbol{b}$ the parameter vector, $y_{i,k}$ the ith experimental observation of the kth response, i.e. the mole fraction of component k (i.e. ammonia, monomethylamine, dimethylamine and trimethylamine), $g_k(\boldsymbol{x}_i, \boldsymbol{b})$ the corresponding value calculated by the model, v the number of responses, n the number of experiments, σ^{kl} the (k, l) element of the inverse of the covariance matrix of the experimental errors on the responses and $\boldsymbol{x}_i$ the vector of the experimental settings corresponding with experiment i. The minimization was achieved by a multi-response Levenberg–Marquardt algorithm [17].

The parameters were evaluated based on their physicochemical significance and tested on their statistical significance on the basis of their individual t-values. The statistical significance of the global regression was expressed by means of the F-test. The adequacy of the mathematical model used for the regression was tested by analysis of the residuals. In order to avoid strong binary correlation between the Arrhenius parameters, the Arrhenius equations were reparametrized according to Kitrell [18]. In this case, 653 K was taken as reference temperature.

6. Thermodynamics

Since the equilibrium position of the transalkylation reactions (1)–(3) is independent of pressure, the transalkylation equilibrium is determined by the temperature and feed composition. The equilibrium coefficients for the transalkylation reactions have been calculated based on thermodynamical data obtained from Reid et al. [19]. As illustrated in Table 1, the calculated values for the equilibrium coefficients differ from those obtained using the experimental correlations given by Issoire and van Long [6]. This discrepancy can be explained by the difference between the values for the standard enthalpy of formation at 298.2 K for dimethyl and trimethylamine given by Gründling et al. [20] and those determined by Issoire and van Long [6] based on experimental data for the equilibrium constants at 673 K.

The calculation of the equilibrium constants based on thermodynamic values was integrated in a Fortran subroutine for determining the equilibrium composition for a given temperature and feed composition. With this subroutine, the equilibrium compositions for all experiments could easily be determined. The following method was applied for a given temperature and feed composition the following linear independent equations can be considered.

N-balance:

$$p_{NH_3} + p_{MMA} + p_{DMA} + p_{TMA} = p^0_{NH_3} + p^0_{MMA} + p^0_{DMA} + p^0_{TMA} \quad (7)$$

C-balance:

$$p_{MMA} + 2p_{DMA} + 3p_{TMA} = p^0_{MMA} + 2p^0_{DMA} + 3p^0_{TMA} \quad (8)$$

where p_i is the partial pressure of component i and p^0_i is the initial partial pressure of component i. If equilibrium is reached, Eqs. (9) and (10) are valid too:

$$K_{eq,1} = \frac{p_{NH_3}p_{DMA}}{p^2_{MMA}} \quad (9)$$

$$K_{eq,2} = \frac{p_{MMA}p_{TMA}}{p^2_{DMA}} \quad (10)$$

Calculation of the partial pressures at equilibrium for a given temperature and feed composition was performed by a single response Levenberg–Marquardt algorithm [17] using Eqs. (7)–(10).

7. Experimental results

Experiments have been performed with pure monomethylamine and dimethylamine and with mixtures of ammonia–monomethylamine, ammonia–dimethylamine and ammonia–trimethylamine. An overview of the investigated total and partial pressures, temperatures and space times is given in Table 2. The partial pressure of nitrogen is not taken into account in the total pressures reported in the paper.

Table 1
Comparison between the equilibrium coefficients for the transalkylation reactions (1)–(3) calculated by thermodynamic data and obtained by Issoire and van Long [6]

Temperature (K)	Obtained by Issoire and van Long			Calculated using thermodynamic data		
	623	653	683	623	653	683
K_1	5.94	4.99	4.25	4.05	3.50	3.07
K_2	2.05	1.82	1.64	1.03	0.96	0.90
K_3	0.08	0.11	0.14	0.24	0.30	0.36

Table 2
Range of experimental conditions

Temperature (K)	623–683
Total pressure (MPa)	0.2–2
Inlet partial pressures (MPa)	
Ammonia	0.3–1.7
Monomethylamine	0.5–1.9
Dimethylamine	0.2–1.8
Trimethylamine	0.2–0.6
Space time ($kg_{cat}\,s\,mol^{-1}$)	2–36

Table 3
Comparison between the product distribution at 1.5 MPa, 653 K and 22.5 kg_{cat} s mol^{-1} for a pure monomethylamine feed and the equilibrium distribution at the same conditions

	Observed distribution (mol%)	Equilibrium distribution (mol%)
Ammonia	32.1	50.8
Monomethylamine	48.7	15.6
Dimethylamine	14.7	16.6
Trimethylamine	4.5	17.0

No equilibrium was reached at the investigated conditions. This is illustrated in Table 3 which compares the effluent composition for a pure monomethylamine feed at 1.5 MPa, 653 K and 22.5 kg_{cat} s mol^{-1} with the calculated equilibrium composition at the same conditions.

The influence of pressure on the conversions depends on the feed composition. For a pure dimethylamine feed at 653 K, the conversion of dimethylamine increases with increasing partial pressure of dimethylamine between 0.2 and 1.5 MPa. The conversion remains constant between 1.5 and 1.8 MPa. This is illustrated in Fig. 2. For a mixture of trimethylamine and ammonia at 653 K, no significant influence of the total pressure was observed between 1 and 1.6 MPa (Fig. 3).

It was observed that when feeding a pure component, even at low conversions (<20%), the effluent contained all three of the methylamines and ammonia. This is illustrated in Fig. 4 for a pure dimethylamine feed at 653 K and 1.8 MPa. The observed product distributions are consistent with an initial reaction rate of monomethylamine equal to the initial reaction rate of trimethylamine. This indicates that

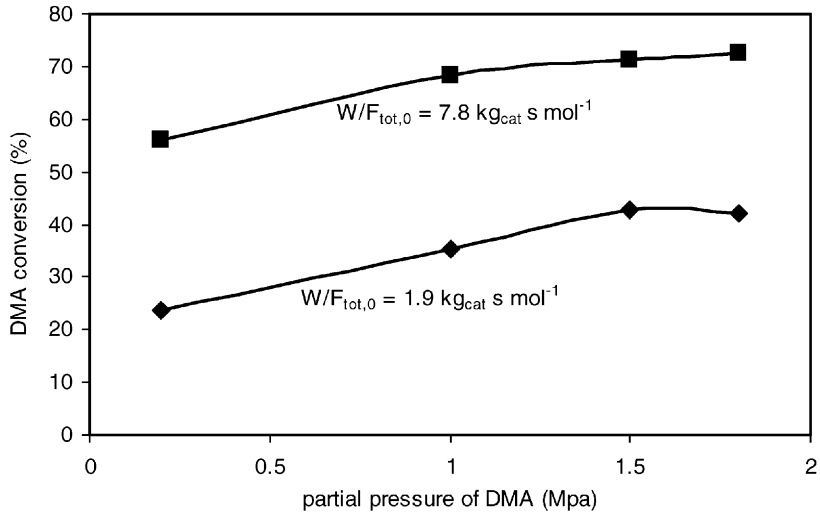

Fig. 2. The observed conversion of dimethylamine (symbols) as a function of the partial pressure of dimethylamine at 653 K: (■) 7.8 and (◆) 1.9 kg_{cat} s mol^{-1}.

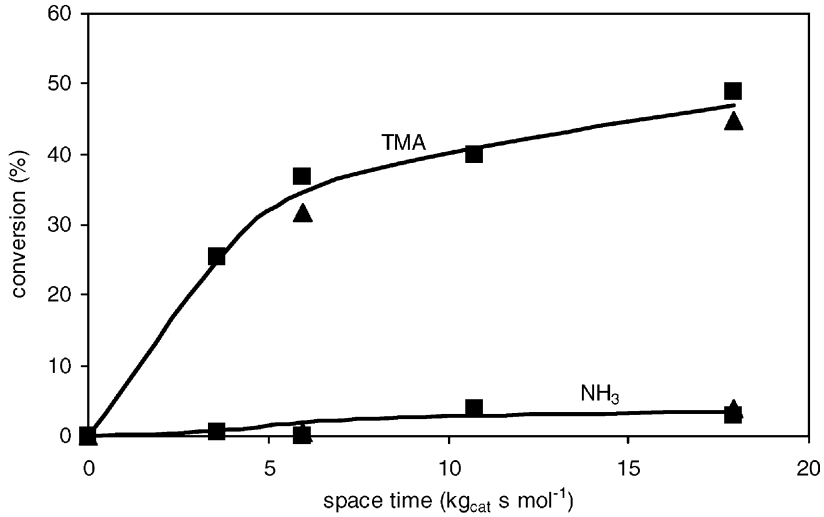

Fig. 3. Observed conversions (symbols) of trimethylamine and ammonia as a function of space time for a feed of trimethylamine and ammonia (N:C = 2:1) at 653 K: (■) 1.6 and (▲) 1 MPa.

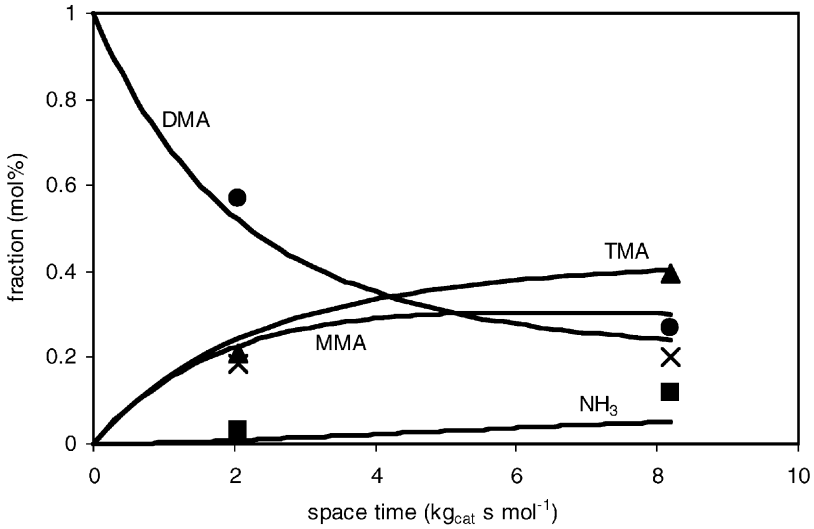

Fig. 4. Observed (symbols) and calculated (lines) product distribution as a function of space time for a pure dimethylamine feed at 653 K and 1.8 MPa: (■) monomethylamine; (●) dimethylamine, (▲) trimethylamine and (◆) ammonia. The calculated mole fractions have been obtained using Eqs. (5) and (12)–(15) with the kinetic parameters of Table 5. Range of experimental conditions, viz. Table 2.

monomethylamine and trimethylamine are primary products of the conversion of dimethylamine by reaction (2). The low mole fractions of ammonia suggest that the latter is a secondary product formed by reactions (1) and/or the reverse of reaction (3).

8. Modeling results

Kinetic modeling was based on elementary reactions. A surface reaction mechanism and a Langmuir adsorption were considered. The reaction paths considered and the corresponding elementary steps are listed in Table 4. The concentration of the surface species were calculated assuming the surface reactions to be rate determining. In combination with the total site balance,

$$C_{\text{tot}} = C^* + C^*_{\text{NH}_3} + C^*_{\text{MMA}} + C^*_{\text{DMA}} + C^*_{\text{TMA}} \tag{11}$$

the reaction rate equations can then simply be written as a function of the partial pressures of the gas phase components, the reaction rate coefficients of the rate determining steps, the equilibrium coefficients of reactions (1)–(3) and the adsorption equilibrium coefficients. In this manner, the following so-called Langmuir–Hinshelwood–Hougen–Watson reaction rate equations were obtained for the reaction paths considered:

$$r_1 = \frac{k_1 K^2_{a,\text{MMA}} (p^2_{\text{MMA}} - p_{\text{DMA}} p_{\text{NH}_3} / K_{\text{eq},1})}{(1 + K_{a,\text{NH}_3} p_{\text{NH}_3} + K_{a,\text{MMA}} p_{\text{MMA}} + K_{a,\text{DMA}} p_{\text{DMA}} + K_{a,\text{TMA}} p_{\text{TMA}})^2} \tag{12}$$

$$r_2 = \frac{k_2 K^2_{a,\text{DMA}} (p^2_{\text{DMA}} - p_{\text{MMA}} p_{\text{TMA}} / K_{\text{eq},2})}{(1 + K_{a,\text{NH}_3} p_{\text{NH}_3} + K_{a,\text{MMA}} p_{\text{MMA}} + K_{a,\text{DMA}} p_{\text{DMA}} + K_{a,\text{TMA}} p_{\text{TMA}})^2} \tag{13}$$

$$r_3 = \frac{k_3 K_{a,\text{NH}_3} K_{a,\text{TMA}} (p_{\text{NH}_3} p_{\text{TMA}} - p_{\text{MMA}} p_{\text{DMA}} / K_{\text{eq},3})}{(1 + K_{a,\text{NH}_3} p_{\text{NH}_3} + K_{a,\text{MMA}} p_{\text{MMA}} + K_{a,\text{DMA}} p_{\text{DMA}} + K_{a,\text{TMA}} p_{\text{TMA}})^2} \tag{14}$$

The net production rates R_i in Eq. (5) can be calculated from the rates of the reaction paths considered in the reaction

Table 4
Elementary steps and reaction paths considered for the kinetic modeling of the transalkylation reactions (1)–(3)

Elementary reactions	Kinetic parameter	Reaction paths		
		1	2	3
$NH_3 + * \rightleftharpoons NH^*_3$	$K_{a,\text{NH3}}$	−1		1
$CH_3NH_2 + * \rightleftharpoons CH_3NH^*_2$	$K_{a,\text{MMA}}$	2	−1	−1
$(CH_3)_2NH + * \rightleftharpoons (CH_3)_2NH^*$	$K_{a,\text{DMA}}$	−1	2	−1
$(CH_3)_3N + * \rightleftharpoons (CH_3)_3N^*$	$K_{a,\text{TMA}}$		−1	1
$2CH_3NH^*_2 \rightleftharpoons NH^*_3 + (CH_3)_2NH^*$	k_1	1		
$2\ (CH_3)_2NH^* \rightleftharpoons CH_3NH^*_2 + (CH_3)_3N^*$	k_2		1	
$NH^*_3 + (CH_3)_3N^* \rightleftharpoons CH_3NH^*_2 + (CH_3)_2NH^*$	k_3			1

Table 5
Parameter estimates with their 95% confidence interval, obtained by regression of 54 data points using Eqs. (5) and (12)–(15)

Kinetic coefficient or adsorption equilibrium coefficient	Reparametrized pre-exponential factor (10^{-1} mol kg_{cat}^{-1} s^{-1}) or (10^{-7} MPa^{-1})	Pre-exponential factor (mol kg_{cat}^{-1} s^{-1})	Activation energy or adsorption enthalpy (10^3 J mol^{-1})
k_1	3.70 ± 1.1	7×10^{18}	241 ± 38
k_2	4.19 ± 1.3	3×10^{16}	210 ± 62
k_3	2.11 ± 0.5	2×10^{10}	138 ± 28
$K_{a,NH3}$	4.06 ± 1.4		−28.2 ± 12
$K_{a,MMA}$	3.68 ± 0.8		−67.1 ± 22
$K_{a,DMA}$	9.84 ± 2.7		−46.7 ± 24
$K_{a,TMA}$	7.12 ± 1.64		−44.0 ± 10

mechanism:

$$R_i = \sum_j v_{i,j} r_j \quad (15)$$

where r_j is the reaction rate of the reaction path j (mol kg_{cat} s^{-1}) and $v_{i,j}$ the stoichiometric coefficient of component i in reaction path j.

Regression of a set of 54 experiments at three temperature levels using Eqs. (5) and (12)–(15) resulted for all parameters in statistically significant estimates. The parameter estimates and their 95% confidence interval are listed in Table 5. The high F-value (=2604) indicates that the model describes the experimental results significantly. The highest binary correlation coefficients (0.955 and 0.948) were observed

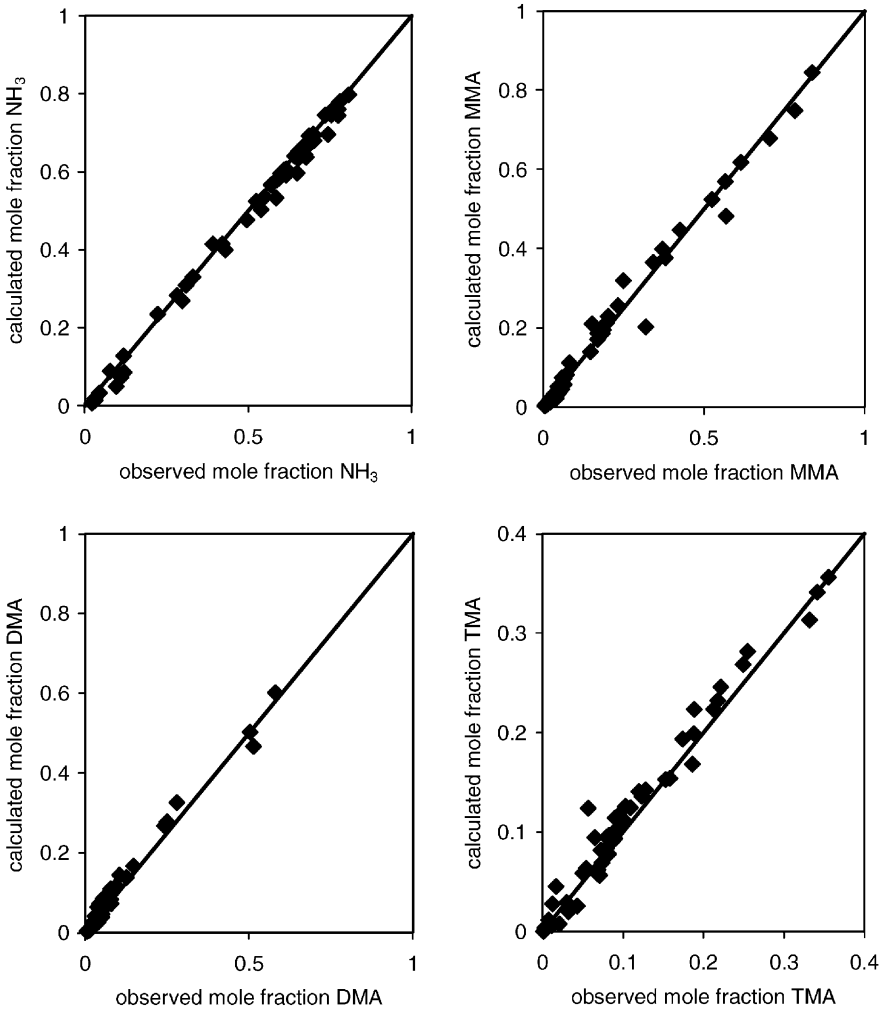

Fig. 5. Parity diagrams for the mole fractions of the transalkylation components. The calculated mole fractions have been obtained using Eqs. (5) and (12)–(15) with the kinetic parameters of Table 5. Range of experimental conditions, viz. Table 2.

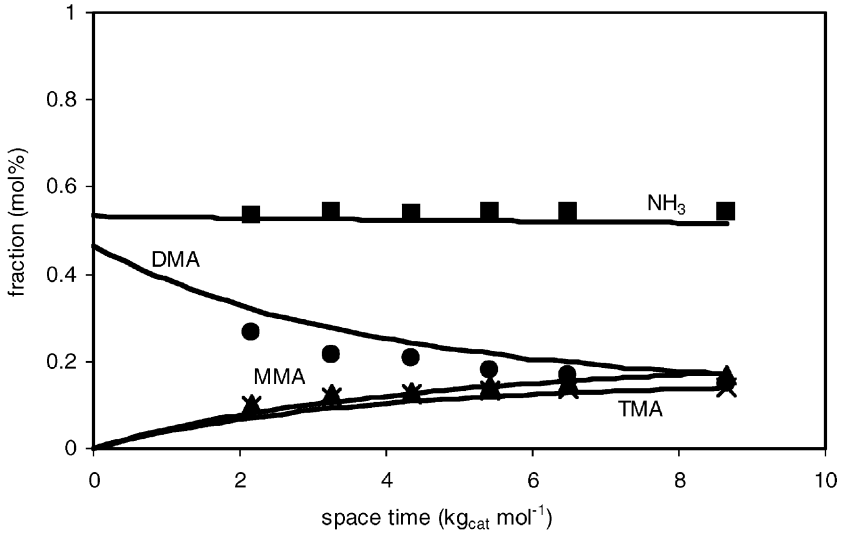

Fig. 6. Experimental (symbols) and simulated (lines) mole fractions as a function of space time for an ammonia–dimethylamine mixture (N/C = 1.1) at 653 K and 1.3 MPa: (■) ammonia; (▲) monomethylamine; (●) dimethylamine and (×) trimethylamine. The calculated mole fractions have been obtained using Eqs. (5) and (12)–(15) with the kinetic parameters of Table 5.

between the reparametrized pre-exponential factors of k_1 and $K_{a,MMA}$ and k_2 and $K_{a,DMA}$, respectively. Fig. 5 shows parity plots for all the experimental data. Modeling the reactor performance with the obtained kinetic parameters resulted in an adequate description of the composition.

Considering a feed of pure dimethylamine, the proposed model predicts equal initial rates for monomethyl and trimethylamine. The initial rate of formation of ammonia is equal to 0. This is in agreement with the experimental observations (Fig. 4).

In Fig. 6 the simulated product distribution is compared with the experimental values at different space times for an ammonia–dimethylamine feed at 1.3 MPa and 653 K. A good agreement between the calculated and the observed values was found. The corresponding fractional surface coverages calculated by the model are shown in Fig. 7. At these conditions the fraction of free sites is approximately 0.6. Even at 1.8 MPa, the fraction of free sites calculated with the model remains comparable to that of the covered ones. Gründling et al. [20], however, report that free Brønsted acid sites were not detected during FTIR experiments on H-mordenite at 633 K and 0.01 MPa. This may be related to a difference in the acid strength of the amorphous catalyst as compared to the zeolite.

As can be seen in Table 5, the reaction rate coefficients k_1 and k_2 at the mean temperature of 653 K, which equal the

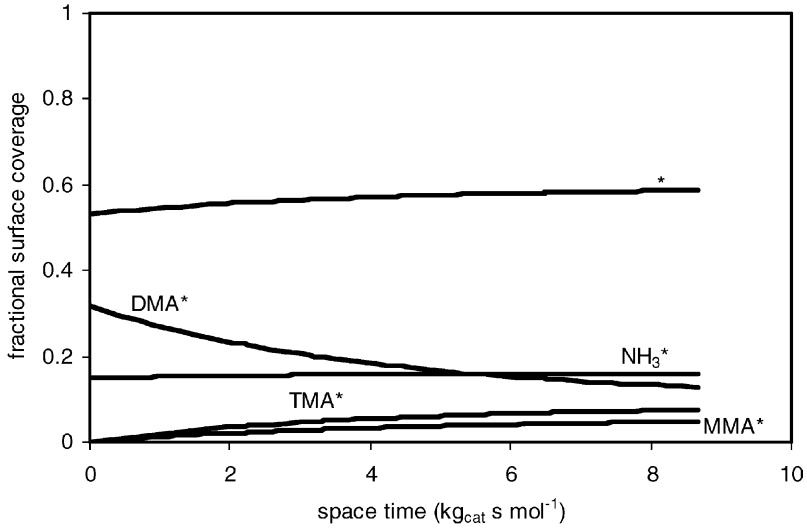

Fig. 7. Simulated fractional surface coverages as a function of space time for an ammonia–dimethylamine mixture (N:C = 1.1:1) at 653 K and 1.3 MPa. Simulated and observed gas phase mole fractions are shown in Fig. 6. The calculated values have been obtained using Eqs. (5) and (12)–(15) with the kinetic parameters of Table 5. (NH_3^*, MMA*, DMA*, TMA*: fractional surface coverage of ammonia, monomethylamine, dimethylamine, trimethylamine, respectively; (∗): fraction free sites).

reparametrized pre-exponential factors of k_1 and k_2, are not significantly different from each other, while k_3 is clearly lower. This agrees with the observations of Issoire and van Long [6] and Mitchel et al. [8] who reported that reaction (3) is the slowest. The estimated activation energies are similar to those given by Mitchell et al. [8].

The estimated pre-exponential factors of the rate coefficients are given in Table 5. The order of magnitude of the pre-exponential factor for Hougen–Watson surface reactions, given by Dumesic et al. [21], ranges from 10^9 to 10^{14} mol kg_{cat}^{-1} s^{-1}, assuming a site density of 10^{19} sites per square meter and taking into account the surface area of 3.52×10^5 m^2 kg^{-1} of the catalyst used. The order of magnitude of the estimated pre-exponential factor of k_3 corresponds then with the range given by Dumesic et al. [21], while the estimated values for the pre-exponential factors of k_1 and k_2 are higher. The estimated adsorption enthalpies are rather low compared with reported literature values for other acidic catalysts. Cardona-Martinez and Dumesic [22] propose adsorption enthalpies of ammonia and trimethylamine on silica-alumina of, approximately -180 and -260 kJ mol^{-1}, respectively. Values for monomethylamine and dimethylamine were not given. The estimated adsorption enthalpies are lower than those for the low-strength adsorption sites on H-ZSM-5 and H-mordenite reported by Chen et al. [23].

Other kinetic models have been considered too. In these models, either methyl scavenging or adsorption-assisted desorption, as discussed by Gründling et al. [20], were considered as rate-determining steps, leading to a linear dependency of the rates on total pressure. However, in the experimental conditions investigated here, this linear dependency was observed for pressures up to about 1.5 MPa only (Fig. 2). Hence, no good model predictions were obtained for the complete range of investigated conditions. However, a good agreement between experimental and calculated values was found between 0.2 and 1.5 MPa with these models. The highest F-value (2146) was obtained for the model with the methyl scavenging reactions as the rate determining steps.

9. Conclusions

The transalkylation reactions have been investigated over a commercial silica-alumina catalyst at industrially relevant conditions. Intrinsic kinetic experiments have been performed between 623 and 683 K, 0.2 and 2 MPa at different space times, for pure component feeds and different feed compositions. A kinetic model for the transalkylation reactions, based on Langmuir adsorption and Hougen–Watson surface reactions was developed. Reaction rate equations have been derived based on the assumption that the surface reactions are rate determining and the adsorption–desorption of ammonia and the methylamines are quasi-equilibrated. Estimation of the kinetic parameters was performed by minimization of the residual sum of squares of the response variables with a multi-response Levenberg–Marquardt algorithm. The obtained parameters were statistically significant and a good agreement between simulated and experimental values was observed. Even at 1.8 MPa, the predicted fraction of free sites was found to be larger than the fraction of the covered ones.

Acknowledgements

The authors would like to acknowledge UCB Chemicals for the financial support.

References

[1] H.C. Foley, D.S. Layfatis, R.K. Mariwala, G.D. Sonnichsen, L.D. Bake, Shape-selective methylamine synthesis: reaction and diffusion in a CMS-SiO_2-Al_2O_3 composite catalyst, Chem. Eng. Sci. 49 (1994) 4771–4786.
[2] M. Deeba, W.J. Ambs, R.N. Cochran, Methanol Amination, US Patent 4,434,300 (1984).
[3] G. Schmitz, Cinétique de la synthèse de la monométhylamine, J. Chim. Phys. 72 (1975) 579–583.
[4] U. Dingerdissen, N. Nagy, F. Fetting, Zur kinetik der Aminierung von methanol an dem zeolith-katalysator ZK-5, Chem. Ing. Tech. 63 (1991) 625–628.
[5] F.J. Weigert, Selective synthesis and equilibration of methylamines on sodium mordenite, J. Catal. 103 (1987) 20–29.
[6] J. Issoire, van Long, Study of the chemical thermodynamics of methylamine formation reactions, C. Bull. Soc. Chim. Fr. 11–12 (1960) 2004.
[7] E. F Restelli, J. Coull, Transmethylation reactions of monomethyl and dimethylamine over montmorillonite in a flow system, AIChE J. 12 (2) (1966) 292.
[8] J.W. Mitchell, K.S. Hayesen, E.G. Lutz, Kinetic study of methylamine reforming over a silica-alumina catalyst, Ind. Eng. Chem. Res. 33 (1994) 181–184.
[9] D.E. Mears, J. Catal. 20 (1971) 127.
[10] G.F. Froment, K. Bischoff, Chemical Reactor Analysis and Design, Wiley, 1990.
[11] J.R. Anderson, K.C. Pratt, Introduction to Characterization and Testing of Catalysts, Academic Press, Sydney, 1985.
[12] D.E. Mears, Chem. Eng. Sci. 26 (1971) 1361.
[13] H. Gierman, Appl. Catal. 43 (1988) 277.
[14] G.D. Byrne, A.C. Hindmarsch, J. Comput. Phys. 70 (1987) 1.
[15] L.R. Petzold, SIAM. J. Stat. Comput. 4 (1983) 136.
[16] Netlib, http://www.netlib.org.
[17] D.W. Marquardt, Ind. Appl. Math. 11 (1963) 431–439.
[18] J.R. Kitrell, Mathematical modelling of chemical reactions, Adv. Chem. Eng. 8 (1970) 97–183.
[19] C. Reid, J.M. Prausnitz, D.E. Poling, The Properties of Gases and Liquids, 4th Edition, McGraw-Hill, New York, 1988.
[20] C. Gründling, G. Eder-Mirth, J.A. Lercher, Surface species in the direct amination of methanol over Brønsted acidic mordenite catalysts, Res. Chem. Int. 23 (1997) 25–40.
[21] J.A. Dumesic, D.F. Rudd, L.M. Aparicio, J.E. Rekoske, A.A. Treviño, The Microkinetics of Heterogeneous Catalysis, American Chemical Society, Washington, DC, 1993.
[22] N. Cardona-Martinez, J. A Dumesic, Microcalorimetric measurements of basic molecule adsorption on silica and silica-alumina, J. Catal. 128 (1991) 23–33.
[23] D.T. Chen, L. Zhang, Yi. Chen, J.A. Dumesic, Dumesic, methylamine synthesis over solid acid catalysts: microcalometric and infrared spectroscopic studies of adsorbed species, J. Catal. 146 (1994) 257–267.